

A FULLY-AUTOMATED SOLVER FOR MULTIPLE SQUARE JIGSAW  
PUZZLES USING HIERARCHICAL CLUSTERING

A Thesis

Presented to

The Faculty of the Department of Computer Science  
San José State University

In Partial Fulfillment

of the Requirements for the Degree

Master of Science

by

Zayd Hammoudeh

December 2016

© 2016

Zayd Hammoudeh

ALL RIGHTS RESERVED

The Designated Thesis Committee Approves the Thesis Titled

A FULLY-AUTOMATED SOLVER FOR MULTIPLE SQUARE JIGSAW  
PUZZLES USING HIERARCHICAL CLUSTERING

by

Zayd Hammoudeh

APPROVED FOR THE DEPARTMENT OF COMPUTER SCIENCE

SAN JOSÉ STATE UNIVERSITY

December 2016

Dr. Chris Pollett      Department of Computer Science

Dr. Thomas Austin      Department of Computer Science

Dr. Teng Moh      Department of Computer Science

## **ABSTRACT**

### **A Fully-Automated Solver for Multiple Square Jigsaw Puzzles Using Hierarchical Clustering**

**by Zayd Hammoudeh**

The square jigsaw puzzle is a variant of traditional jigsaw puzzles, wherein all pieces are equal-sized squares; these pieces must be placed adjacent to one another to reconstruct an original image. This thesis proposes a novel solver based on hierarchical clustering that can reconstruct multiple square jigsaw puzzles simultaneously without any information beyond the set of puzzle pieces. This algorithm has been verified on up to 10 puzzles simultaneously, which is more than double the current state of the art.

This thesis also defines the first set of metrics specifically tailored for multiple puzzle solvers. This thesis also outlines the first visualization standards for representing the quality of solver solutions.

## **DEDICATION**

To my mother.

## TABLE OF CONTENTS

### CHAPTER

<b>1</b>	<b>Introduction</b>	<b>1</b>
<b>2</b>	<b>Previous Work</b>	<b>3</b>
<b>3</b>	<b>Mixed-Bag Solver Overview</b>	<b>7</b>
3.1	Assembly	7
3.1.1	Assembler Time Complexity	8
3.1.2	Assembler Implementation	9
3.2	Segmentation	9
3.2.1	Overview of the Segmentation Procedure	10
3.2.2	Partitioning into a Puzzle into Segments	10
3.2.3	Articulation Points	12
3.3	Stitching	13
3.3.1	Mini-Assemblies and Stitching Pieces	14
3.3.2	Selection of Stitching Pieces	14
3.3.3	Quantifying Inter-Segment Relationships	17
3.4	Hierarchical Clustering of Segments	18
3.4.1	Calculating the Initial Similarity Matrix	19
3.4.2	Updating the Similarity Matrix via Single Linking	19
3.4.3	Terminating Hierarchical Clustering	20
3.5	Final Seed Piece Selection	20
3.6	Final Assembly	21

<b>4 Quantifying and Visualizing the Quality of a Mixed-Bag Solver Output</b>	22
4.1 Direct Accuracy	22
4.1.1 Enhanced Direct Accuracy Score	23
4.1.2 Shiftable Enhanced Direct Accuracy Score	24
4.1.3 Necessity of Using Both EDAS and SEDAS	26
4.2 Neighbor Accuracy	26
4.2.1 Enhanced Neighbor Accuracy Score	27
4.3 Best Buddy Metrics	27
4.3.1 Interior and Exterior Best Buddies	28
4.3.2 Best Buddy Density	28
4.4 Visualizing Solver Output Quality and Best Buddies Relationships	29
4.4.1 Visualizing EDAS and SEDAS	29
4.4.2 Visualizing ENAS	30
4.4.3 Visualizing Best Buddies	32
<b>5 Experimental Results</b>	34
5.1 Accuracy Determining the Number of Input Puzzles	35
5.1.1 Single Puzzle Solving	35
5.1.2 Multiple Puzzle Solving	37
5.2 Comparison of Solver Output Quality	38
5.3 Ten Puzzle Solving	39
<b>6 Conclusions and Future Work</b>	42
<b>LIST OF REFERENCES</b>	44

## **APPENDIX**

<b>A Example Output of a Single Segmentation Round . . . . .</b>	<b>47</b>
<b>B Incorrectly Classified Single Puzzle Images . . . . .</b>	<b>50</b>
<b>C Ten Puzzle Results . . . . .</b>	<b>53</b>

## LIST OF TABLES

1	Color Scheme for Puzzles Pieces in Direct Accuracy Visualizations	30
2	Color Scheme for Puzzles Piece Sides in Neighbor Accuracy Visualizations . . . . .	31
3	Color Scheme for Puzzles Piece Sides in Best Buddy Visualizations	33
4	Number of Solver Iterations for Each Puzzle Input Count . . . . .	35
5	Comparison of Mixed-Bag and Paikin & Tal Solvers Performance on Multiple Input Puzzles . . . . .	38
6	Comparison of the Image Shifting, SEDAS, and ENAS Results for the 10 Puzzle Dataset . . . . .	40

## LIST OF FIGURES

1	Jig Swap Puzzle Example . . . . .	2
2	Relationship between the Mixed-Bag Solver’s Components . . . . .	7
3	Solver Output where a Single Misplaced Piece Catastrophically Affects the Direct Accuracy . . . . .	25
4	Example Solver Output Visualizations for EDAS and SEDAS . .	31
5	Example Solver Output Visualization for ENAS . . . . .	32
6	Visualization of Best Buddies in an Image . . . . .	33
7	Comparison of Best Buddy Density and Interior Non-Adjacent Best Buddies for Two Images from the Pomeranz <i>et al.</i> 805 Piece Dataset	36
8	Mixed-Bag Solver’s Input Puzzle Count Error Frequency . . . . .	37
9	Performance of the Mixed-Bag and Paikin & Tal Solvers with Multiple Input Puzzles . . . . .	41
A.10	Ground-Truth Images Used in the Segmentation Example . . . . .	48
A.11	Example Assembler Output of a Single Puzzle after the First Segmentation Round . . . . .	48
A.12	Segmentation of the Assembler Output with Coloring for Distance to the Nearest Open and Marking of the Articulation Points . .	49
A.13	Best Buddy Visualization of the Assembler Output . . . . .	49
B.14	805 Piece Images that were Incorrectly Identified by the Mixed Bag Solver . . . . .	51
B.15	Multi-Bag Solver Outputs for the Images not Correctly Identified as Single Inputs . . . . .	52
C.16	First Set of Six Images Comprising the 10 Image Test Set . . . . .	54
C.17	Second Set of Four Images Comprising the 10 Image Test Set . .	55
C.18	First Set of Six Mixed-Bag Solver Images for the 10 Image Test Set	56

C.19	Second Set of Four Mixed-Bag Solver Images for the 10 Image Test Set . . . . .	57
C.20	First Set of Six SEDAS Visualizations for the 10 Image Test Set . . . . .	58
C.21	Second Set of Four SEDAS Visualizations for the 10 Image Test Set . . . . .	59

## CHAPTER 1

### Introduction

Jigsaw puzzles were first introduced in the 1760s when they were made from wood. The name “jigsaw” derives from the jigsaws that were used to carve the wooden pieces. The 1930s saw the introduction of the modern jigsaw puzzle where an image was printed on a cardboard sheet that was cut into a set of interlocking pieces [1, 2]. Although jigsaw puzzles had been solved by children for more than two centuries, it was not until 1964 that the first automated jigsaw puzzle solver was proposed by Freeman & Gardner [3]. While an automated jigsaw puzzle solver may seem trivial, the problem has been shown by Altman [4] and Demaine & Demaine [5] to be strongly NP-complete when pairwise compatibility between pieces is not a reliable metric for determining adjacency.

Jig swap puzzles are a specific type of jigsaw puzzle where all pieces are equal sized, non-overlapping squares.<sup>1</sup> An example of a jig swap puzzle is shown in Figure 1. Jig swap puzzles are substantially more challenging to solve than traditional jigsaw puzzles since piece shape cannot be considered when determining inter-piece affinity. Rather, only the image information on each individual piece is used when solving the puzzle.

There are clear parallels between the jigsaw puzzle problem and other domains where an object must be reconstructed from a set of component pieces. As such, techniques developed for jigsaw puzzles can often be generalized to many practical problems. Some example applications of jigsaw puzzle solving techniques are:

---

<sup>1</sup>Unless otherwise noted, the phrase “jigsaw puzzle” is used in this thesis to refer to specifically jig swap puzzles.



(a) Ground-Truth Image



(b) Randomized Jig Swap Puzzle

Figure 1: Jig Swap Puzzle Example

reassembly of archaeological artifacts [6, 7], forensic analysis of deleted files [8], image editing [9], reconstruction of shredded documents [10], DNA fragment reassembly [11], and speech descrambling [12]. In most of these practical applications, the original, also known as “ground-truth,” input is unknown. This significantly increases the difficulty of the problem as the structure of the complete solution must be determined solely from the bag of component pieces.

This thesis describes a fully-automated solver for the simultaneous assembly of multiple jigsaw puzzles. Unlike previous solvers, the algorithm presented here does not require any information beyond the set of puzzle pieces. What is more, this thesis defines a set of new metrics specifically tailored for quantifying the quality of outputs of multiple puzzle solvers. Lastly, this thesis outlines a set of standards for visualizing the characteristics of solver outputs.

## CHAPTER 2

### Previous Work

Computational jigsaw puzzle solvers have been studied since the 1960s when Freeman & Gardner proposed a solver that relied only on piece shape and could solve puzzles with up to nine pieces [3]. Since then, the focus of research has gradually shifted from traditional jigsaw puzzles to jig swap puzzles.

Cho *et al.* [13] proposed in 2010 one of the first modern computational jig swap puzzle solvers; their approach relied on a graphical model built around a set of one or more “anchor piece(s),” which are pieces whose position is fixed in the correct location before the solver begins. Their solver also required that the user specify the actual dimensions of the input puzzle. Future solvers would improve on Cho *et al.*’s results while simultaneously reducing the amount of information (i.e., beyond the set of pieces) passed to the solver.

A significant contribution of Cho *et al.* is that they were first to use the LAB (Lightness and the A/B opponent color dimensions) colorspace to encode image pixels. LAB was selected due to its property of normalizing the lightness and color variation across all three pixel dimensions. Cho *et al.* also proposed a measure for quantifying the pairwise distance between two puzzle pieces that became the basis of most future work.

Pomeranz *et al.* [14] proposed an iterative, greedy, jig swap puzzle solver in 2011. Their approach did not rely on anchor pieces, and the only information passed to the solver were the pieces, their orientation, and the dimensions of the puzzle. Pomeranz *et al.* also generalized and improved on Cho *et al.*’s inter-piece pairwise

distance measure by proposing a “predictive distance measure.” Finally, Pomeranz *et al.* introduced the concept of “best buddies.” Equation 1 formally defines the best buddy relationship between the side (e.g., top, left, right, bottom),  $s_x$ , of puzzle piece,  $p_i$ , and the side,  $s_y$ , of piece  $p_j$ . Note that  $C(p_i, s_x, p_j, s_y)$  represents the compatibility between the two piece’s respective sides.

$$\forall x_k \forall s_c, C(x_i, s_a, x_j, s_b) \geq C(x_i, s_a, x_k, s_c) \quad \text{and} \quad (1)$$

$$\forall x_k \forall s_c, C(x_j, s_b, x_i, s_a) \geq C(x_j, s_b, x_k, s_c)$$

Best buddies have served as both as metric for estimating the quality of a solver output [15] as well as the foundation of some solvers’ assemblers [16]. Best buddies are discussed extensively in sections 3.2.2, 4.3 and 5.1.1 of this thesis.

An additional key contribution of Pomeranz *et al.* is the creation of three image benchmarks. The first benchmark is comprised of twenty, 805 piece images; this benchmark is used as the test set for the experiments described in Chapter 5. The other two benchmarks each consist of three images; the first dataset has images containing 2,360 pieces while the other consists of images with 3,300 pieces.

In 2012, Gallagher [17] formally categorized jig swap puzzle problems into four primary types. The following is Gallagher’s proposed terminology; his nomenclature is used throughout this thesis.

- **Type 1 Puzzle:** The dimensions of the puzzle (i.e., the width and height of the ground-truth image in number of pixels) is known. The orientation/rotation of each piece is also known, which means that there are exactly four pairwise relationships between any two pieces. At a minimum, the solver is provided

with the correct location of a single “anchor” piece, with additional anchor pieces being optional. This type of puzzle is the focus of [13, 14].

- **Type 2 Puzzle:** This is an extension of a Type 1 puzzle, where pieces may be rotated in  $90^\circ$  increments (e.g.,  $0^\circ$ ,  $90^\circ$ ,  $180^\circ$ , or  $270^\circ$ ); in comparison to a Type 1 puzzle, this change alone increases the number of possible solutions by a factor of  $4^n$ , where  $n$  is the number of puzzle pieces. What is more, no piece locations are known in advance, which means there are anchor pieces. Lastly, the dimensions of the ground-truth image may be unknown.
- **Type 3 Puzzle:** All puzzle piece locations are known and only the rotation of the pieces is unknown. This is the least computationally complex of the puzzle variants and is generally considered the least interesting. Type 3 puzzles are not explored as part of this thesis.
- **Mixed-Bag Puzzles:** The input set of pieces are from multiple puzzles. The solver may output either a single, merged puzzle, or it may separate the puzzle pieces into disjoint sets that ideally align with the set of ground-truth input images. This type of puzzle is the primary focus of this thesis.

In 2013, Sholomon *et al.*[15] proposed a genetic algorithm-based solver for Type 1 puzzles. By moving away from the greedy approach used by Pomeranz *et al.*, Sholomon *et al.*’s approach is more immune to suboptimal decisions early in the placement process. Sholomon *et al.*’s algorithm is able to solve puzzles of significantly larger size than previous techniques (e.g., greater than 23,000 pieces). What is more, Sholomon *et al.* defined three new large image benchmarks; the specific puzzle sizes are 5,015, 10,375, and 22,834 pieces [18].

Paikin & Tal [16] published in 2015 a greedy solver that handles both Type 1 and Type 2 puzzles, even if those puzzles are missing pieces. What is more, their algorithm is one of the first to support Mixed-Bag Puzzles. While Paikin & Tal’s algorithm represents the current state of the art, it has serious limitations that affects its performance for Mixed-Bag puzzles. For example, similar to previous solvers, Paikin & Tal’s algorithm must be told the number of input puzzles. In many practical applications, this information may not be known.

Another limitation arises from the fact that Paikin & Tal’s algorithm places pieces using a single-pass kernel growing approach. As such, a single piece is used as the seed of each output puzzle, and all subsequent pieces are placed around the expanding kernel. Because of that, poor seed selection can catastrophically degrade the quality of the solver output. However, their algorithm only requires that a seed piece have best buddies on each of its sides and that each of the seed’s best buddies also have best buddies on each of their sides. Therefore, the selection of the seed is based off essentially 13 pieces. Since so few pieces determine the choice of a seed, it is common that the seeds of multiple output puzzles come the same ground-truth image.

The limitations of Paikin & Tal’s algorithm are addressed by this thesis’ Mixed-Bag Solver, which is described in Chapter 3. Since Paikin & Tal’s algorithm represents the current state of the art, it is used as thesis’ assembler. What is more, their algorithm is used as the baseline for all performance comparisons.

## CHAPTER 3

### Mixed-Bag Solver Overview

When humans solves jigsaw puzzles, it is common that they first correctly assemble small regions of the puzzle and then merge those smaller regions to form larger regions. The Mixed-Bag Solver presented in this thesis is based of this solving strategy. The solver consists of five distinct stages, namely: segmentation, stitching, hierarchical clustering of segments, seed piece selection, and final assembly. The flow of the algorithm is shown in Figure 2; the pseudocode for the solver, including the input(s) and output of each stage is shown in Algorithm 1. The techniques used by the Mixed-Bag Solver are valid for Type 1, Type 2, and Mixed-Bag puzzles.

The following subsections describe each of Mixed-Bag Solver's stages/subfunctions. It also discusses the assembler (not shown in Figure 2), which is a separate but associated component of the architecture.

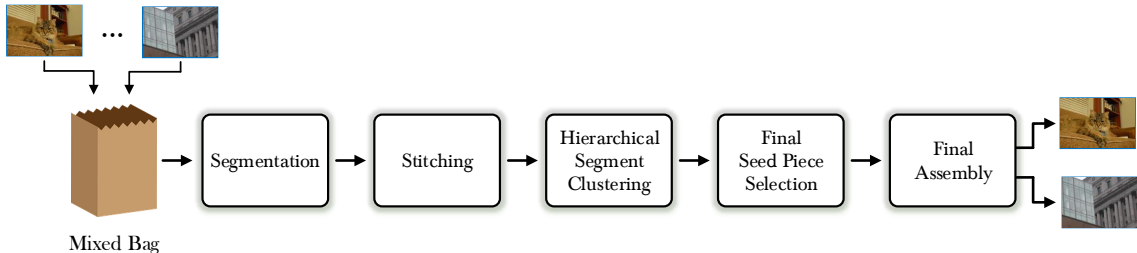


Figure 2: Relationship between the Mixed-Bag Solver's Components

#### 3.1 Assembly

The assembler places the individual pieces in the solved puzzle. The Mixed-Bag Solver's architecture is largely independent of the particular assembler used. Hence, any improvements or modifications to the assembler can be directly incorporated into

---

**Algorithm 1** Pseudocode for the Mixed-Bag Solver

---

```
1: function MIXEDBAGSOLVER(puzzle_pieces)
2:   saved_segments  $\leftarrow$  SEGMENTATION(puzzle_pieces)
3:   overlap_matrix  $\leftarrow$  STITCHING(saved_segments, puzzle_pieces)
4:   clusters  $\leftarrow$  HIERARCHICALCLUSTERING(saved_segments, overlap_matrix)
5:   puzzle_seed_pieces  $\leftarrow$  FINDSEEDPIECES(clusters)
6:   solved_puzzles  $\leftarrow$  RUNFINALASSEMBLY(puzzle_seed_pieces, puzzle_pieces)
7:   return solved_puzzles
```

---

the Mixed-Bag Solver to improve the solver’s performance. What is more, if particular assemblers perform better for particular applications, the assemblers can be interchanged. This provides the Mixed-Bag Solver with significant flexibility and upgradability to maximize performance across a wide range of applications.

This thesis uses the assembler proposed by Paikin & Tal [16] for all experiments. As mentioned in Chapter 2, their assembler is the current state of the art and is one of the few algorithms that natively supports Mixed-Bag puzzles.

### 3.1.1 Assembler Time Complexity

Paikin & Tal’s assembler relies on a set of inter-puzzle piece similarity metrics. Similar to all other jig swap solvers, these distances are calculated between all pairs of pieces, make the time required to calculate inter-piece similarity  $O(n^2)$ , where  $n$  is the number of puzzle pieces. If an input image has sufficient inter-piece variation, then the placement of all puzzle pieces is  $\Theta(n \lg(n))$ , as a heap is used to determine the next piece to be placed. However, if most pieces are sufficiently similar that there are relatively few best buddies (see Chapter 2), then piece placement can be as slow as  $O(n^3)$  as the inter-piece similarity may need to be recalculated after each piece is placed.

The Mixed-Bag Solver performs assembly at least once during the segmentation

stage (usually more times) and must be repeated during the final assembly stage. Hence, while the execution time for the Mixed-Bag solver is longer than the assembler itself, they both share the same time complexity since the number of times placement must be performed is not dependent on the number of puzzle pieces.

### 3.1.2 Assembler Implementation

Paikin & Tal wrote their algorithm in Java, and as of this publication, the source code has not been released. Hence, their algorithm was reimplemented as part of this thesis using the description in [16]. This thesis' implementation is written in the Python programming language and is fully open-source. No execution time comparisons between their algorithm and the Mixed-Bag Solver are included with this thesis since Java is generally significantly faster than Python [19].

## 3.2 Segmentation

Segmentation provides basic structure to the bag of puzzle pieces by partitioning these pieces into disjoint sets, referred to here as segments. These segments are partial assemblies where there is a high degree of confidence that the pieces are placed correctly. As detailed in Algorithm 1, the only input to the segmentation stage is the bag of puzzle pieces itself; the solver takes no other inputs. It is expected that pieces from the same input puzzle may be assigned to multiple disjoint segments. Section 3.4 describes how these segments are merged using hierarchical clustering.

### 3.2.1 Overview of the Segmentation Procedure

Algorithm 2 outlines the basic segmentation framework; the implementation is iterative and will have one or more rounds. In each round, all pieces not yet assigned to a saved segment are assembled as if they all belong to a single ground-truth image. This strategy eliminates the need to make any assumptions at this early stage regarding the number of input puzzles.

Section 3.2.2 describes the procedure used to create the individual segments. The largest segment in each round is passed to the Stitching stage described in Section 3.3.<sup>1</sup> Similarly, the multiplicative scalar term “ $\alpha$ ” in Algorithm 2 dictates which other segments are also passed to the Stitching stage. In this thesis,  $\alpha$  was set to 0.5, meaning that all segments that are at least half the size of the largest segment are also saved. This approach provided sufficient balance between finding the largest possible segments while limiting overall execution time.

Once a piece is assigned to a saved segment, it is removed from the set of unassigned pieces. Hence, those pieces will not be placed in the future segmentation rounds. Segmentation continues until all pieces have been assigned to sufficiently large segments, or no segment exceeds the minimum allowed segment size.

### 3.2.2 Partitioning into a Puzzle into Segments

The function “SEGMENTPUZZLE” in Algorithm 3 partitions a solved puzzle into disjoint segments. The procedure is adapted from the kernel growing segmentation algorithm proposed by Pomeranz *et al.*, where it was shown to have greater than 99.7% accuracy identifying genuine neighbors [14].

---

<sup>1</sup>All saved segments must exceed a minimum size. For this thesis, it was observed that a minimum segment size of 7 provided the best balance between solution quality and algorithm execution time.

---

**Algorithm 2** Pseudocode for the Complete Segmentation Algorithm

---

```
1: function SEGMENTATION(puzzle_pieces)
2:   saved_segments  $\leftarrow \{\}$ 
3:   unassigned_pieces  $\leftarrow \{puzzle\_pieces\}$ 
4:   loop
5:     solved_puzzle  $\leftarrow$  RUNSINGLEPUZZLEASSEMBLY(unassigned_pieces)
6:     puzzle_segments  $\leftarrow$  SEGMENTPUZZLE(solved_puzzle)
7:     max_segment_size  $\leftarrow$  maximum size of segment in puzzle_segments
8:     if max_segment_size < smallest_allowed then
9:       return saved_segments
10:      for each segment  $\in$  puzzle_segments do
11:        if  $|segment| > \alpha \times max\_segment\_size$  and  $|segment| > 0$  then
12:          add segment to saved_segments
13:          remove pieces in segment from unassigned_pieces
```

---

When each new segment is created, a single seed piece is added. Whenever any piece, including the seed, is added to a segment, the algorithm examines all of that piece’s neighbors. These adjacent pieces are also added to the segment if they are in the pool of unassigned pieces and if their neighbor inside the segment is a “best buddy” (as determined by the predicate ISBESTBUDDIES). The growth of a segment terminates when there are no neighboring pieces that satisfy these two criteria.

In Pomeranz *et al.*’s algorithm, no changes were made to a segment after it reached its maximum size. Their approach is sufficient when solving only a single puzzle at a time. However, in Mixed-Bag puzzles, it is common that correctly assembled regions from different ground-truth inputs are joined into a single segment by very tenuous linking, usually in the form of narrow bridges no wider than a single piece. As described in the next section, the Mixed-Bag Solver post processes each segment after it has grown to its maximum size to prevent erroneous segment merging.

---

**Algorithm 3** Pseudocode for Segmenting a Solved Puzzle

---

```
1: function SEGMENTPUZZLE(solved_puzzle)
2:   puzzle_segments  $\leftarrow \{\}$ 
3:   unassigned_pieces  $\leftarrow \{\text{all pieces in } solved\_puzzle\}$ 

4:   while  $|\text{unassigned\_pieces}| > 0$  do
5:     segment  $\leftarrow$  new empty segment
6:     seed_piece  $\leftarrow$  next piece in unassigned_pieces
7:     queue  $\leftarrow [seed\_piece]$ 

8:     while  $|\text{queue}| > 0$  do
9:       piece  $\leftarrow$  next piece in queue
10:      add piece to segment

11:     for each neighbor_piece of piece do
12:       if ISBESTBUDDIES(neighbor_piece, piece) then
13:         add neighbor_piece to queue
14:         remove neighbor_piece from unassigned_pieces

15:     articulation_points  $\leftarrow$  FINDARTICULATIONPOINTS(segment)
16:     remove articulation_points from segment

17:     disconnected_pieces  $\leftarrow$  FINDDISCONNECTEDPIECES(segment)
18:     remove disconnected_points from segment

19:     add articulation_points and disconnected_pieces to unassigned_pieces
20:     add segment to puzzle_segments

21:   return puzzle_segments
```

---

### 3.2.3 Articulation Points

A segment can be modeled as a graph with a single connected component. The individual puzzle pieces represent the vertices while the edges are the best buddy relationships between adjacent pieces. An articulation point is any vertex (i.e., puzzle piece) in the graph whose removal increases the number of connected components. The Mixed-Bag Solver identifies the articulation points using the algorithm proposed

by [20]; these articulation pieces are then removed from the segment and returned to the set of unassigned pieces. This necessarily causes some other pieces to become disconnected from the segment’s seed. Any disconnected pieces are also removed from the segment and marked as unassigned.

### 3.3 Stitching

As discussed previously, a segment represents an ordering of pieces where there is a particularly high degree of confidence that the placement is correct. In some areas of an image (e.g., a sky where there is little variation between pieces), the segmenter may not have high confidence that the puzzle is assembled correctly. This often leads to a single ground-truth image being comprised of multiple segments. Since the Mixed-Bag Solver is not supplied with the number of input puzzles, it must quantify the extent to which any pairs of segments are related to ensure it can accurately estimate the number of ground-truth inputs.

It is expected that two segments that were adjacent in a ground-truth image would eventually merge if one segment were allowed to expand. Since it is not known in which relative direction adjacent segment(s) may be located, the segment should be allowed to grow in all directions; however, the segment should not be forced to expand in a certain direction as it may lead to the formation of erroneous inter-segment coupling. This concept serves as the foundation of the inter-segment stitching used by the Mixed-Bag Solver. The stitching process is described in the following subsections.

### **3.3.1 Mini-Assemblies and Stitching Pieces**

As mentioned previously, a segment should be allowed, but not forced, to expand in all directions in order to identify related segments. To achieve this, the Mixed-Bag Solver introduces the concept of a “mini-assembly,” which is similar to the standard assembly process described in Section 3.1 with the expectation that only a limited number of pieces are placed.<sup>2</sup> The seeds for each of these mini-assemblies is referred to as a “stitching piece” since they serve the role of “stitching” together associated segments.

### **3.3.2 Selection of Stitching Pieces**

If stitching pieces are poorly selected, two negative, yet divergent outcomes may happen. First, placing the stitching pieces too close to one another can add significant overhead without creating much tangible value. In contrast, if the stitching pieces are too far apart, the solver may not be able to detect subtle inter-segment relationships. Algorithm 4 describes the procedure used by the Mixed-Bag Solver to select the stitching pieces that balances these two concerns. The implementation of this algorithm is described in detail in the following two subsections.

#### **3.3.2.1 Spacing the Stitching Pieces from Open Locations**

It is not sufficient for stitching pieces to be placed solely around the external perimeter of a segment as it is common for segments to have internal voids, where no pieces are present. As such, stitching pieces are placed near “open locations,” which are all valid puzzle locations that have either a piece from a different segment or no piece at all. If a stitching piece is too close to one of these open locations, erroneous

---

<sup>2</sup>In this thesis, a mini-assembly places exactly 100 pieces.

---

**Algorithm 4** Pseudocode for Selecting the Stitching Pieces in a Segment

---

```
1: procedure FINDSTITCHINGPIECES(segment_pieces)
2:   FINDPIECEDISTANCETOOPEN(segment_pieces)
3:   segment_stitching_pieces  $\leftarrow \{\}$ 
4:   segment_grid_cells  $\leftarrow$  PARTITIONINTOGGRID(segment)
5:   for each grid_cell  $\in$  segment_grid_cells do
6:     if HASPIECEADJACENTTOOPEN(grid_cell) then
7:       candidates  $\leftarrow \{pieces\} \in grid_cell closest to target distance_to_open
8:       stitching_piece  $\leftarrow$  piece  $\in$  candidates closest to center of grid_cell
9:       add stitching_piece to segment_stitching_pieces
10:  return segment_stitching_pieces$ 
```

---

coupling between unrelated segments may occur. Algorithm 4 invokes the function FINDPIECEDISTANCETOOPEN to determine the distance of each piece in the segment to the nearest open location; the implementation of this function is shown in Algorithm 5.

FINDPIECEDISTANCETOOPEN follows an iterative boundary tracing technique; hence, during each iteration of the **while** loop on line 5, all segment pieces whose distance to the nearest open location is equal to *distance\_to\_open* are explored. Therefore, any pieces explored in the first iteration of the **while** loop have a distance of 1 to the nearest open while those explored in the second iteration have distance 2, etc. There are two primary reasons this thesis uses iterative boundary tracing here. First, the algorithm is robust enough to handle internal voids as well as potential necking within the segment where two large segment components are joined by a narrower bridge. What is more, since each piece is explored only once, the execution time of this algorithm is  $O(n)$ , where  $n$  is the number of pieces in the segment.

---

**Algorithm 5** Pseudocode for Determining the Manhattan Distance between Each Segment Piece and the Nearest Open Location

---

```
1: procedure FINDPIECEDISTANCETOOPEN(segment_pieces)
2:   explored_pieces  $\leftarrow \{\}$ 
3:   locations_at_prev_dist  $\leftarrow \{\text{open locations adjacent to } segment\_pieces\}$ 
4:   distance_to_open  $\leftarrow 1$ 

5:   while  $|\text{explored\_pieces}| > 0$  do
6:     locations_at_current_dist  $\leftarrow \{\}$ 

7:     for each prev_dist_loc  $\in \text{locations\_at\_prev\_dist}$  do
8:       for each adjacent_loc of prev_dist_loc do
9:         if  $\exists \text{piece at } adjacent\_loc \text{ and } piece \notin \text{explored\_pieces}$  then
10:          set distance_to_open for piece
11:          add piece to explored_pieces
12:          add adjacent_loc to locations_at_current_dist

13:     locations_at_prev_dist  $\leftarrow \text{locations\_at\_current\_dist}$ 
14:     distance_to_open  $\leftarrow \text{distance\_to\_open} + 1$ 
```

---

### 3.3.2.2 Spacing between Stitching Pieces

If stitching pieces are too close together, the outputs from several mini-assemblies will be almost identical, which implies that the additional stitching pieces added little value. To address inter-stitching piece spacing, Algorithm 4 sub-partitions each segment into a grid of adjacent cells; this allows the algorithm to easily space out the stitching pieces at some maximum spacing. The grid spans the entire segment starting from the piece in the upper left corner of the segment. For this thesis, the grid cell width was set to 10 pieces.<sup>3</sup>

Stitching pieces will only be selected from those grid cells that have at least one puzzle piece adjacent to an open location. For such grid cells, the algorithm finds the

---

<sup>3</sup>If the segment dimensions are not evenly divisible by the target cell width, grid cells along the bottom and right boundaries of the segment will be narrower than the specified target.

set of pieces (if any) whose distance to the nearest open location equals the target.<sup>4</sup> If no pieces satisfy that criteria, then the target value is decremented until at least one piece is identified. From amongst the set of candidates that satisfy the open distance to location criteria, the piece that is closest to center of the grid cell is selected for stitching.

### 3.3.3 Quantifying Inter-Segment Relationships

As mentioned previously, a mini-assembly will be performed for each stitching piece  $\zeta_x$  in segment  $\Phi_i$  where  $\zeta_x \in \Phi_i$ . The output from this mini-assembly,  $MA_{\zeta_x}$ , will contain puzzle pieces from one or more segments. If the solver output includes pieces from a different segment, there is a significantly increased likelihood that the two segments came from the same ground-truth input.

Equation (2) defines the overlap between segment,  $\Phi_i$ , and any other segment,  $\Phi_j$ . The intersection between the mini-assembly output and segment  $\Phi_j$  needs is normalized with respect to both the number of pieces in mini-assembly as well as potentially the size of segment  $\Phi_j$ , since the latter will dictate the maximum overlap if  $|\Phi_j| < |MS_{\zeta_x}|$ .

$$Overlap_{\Phi_i, \Phi_j} = \arg \max_{\zeta_x \in \Phi_i} \frac{|MS_{\zeta_x} \cap \Phi_j|}{\min(|MS_{\zeta_x}|, |\Phi_j|)} \quad (2)$$

The outputs of the mini-assemblies will vary between segments based off their respective stitching pieces as well as potentially the size of the segments. Hence, in most cases, the overlap coefficient is asymmetric meaning:

$Overlap_{\Phi_i, \Phi_j} \neq Overlap_{\Phi_j, \Phi_i}$ . Section 3.4.1 defines how the overlap coefficients are normalized to quantify inter-segment similarity.

---

<sup>4</sup>For this thesis, the target distance to the nearest open location was set to 3.

---

**Algorithm 6** Pseudocode for the Hierarchical Clustering of Segments

---

```
1: function HIERARCHICALCLUSTERING(solved_segments, overlap_matrix)
2:   segment_clusters = {}
3:   for each segmenti ∈ solved_segments do
4:     add new segment cluster  $\Phi_i$  containing segmenti to segment_clusters
5:   Compute the similarity matrix  $\Gamma$  from overlap_matrix
6:   while maximum similarity in  $\Gamma > \text{min\_cluster\_similarity}$  do
7:     Merge the two most similar clusters  $\Phi_i$  and  $\Phi_j$  in segment_clusters
8:     Update the similarity matrix,  $\Gamma$  for the merged clusters
9:   return cluster_segments
```

---

### 3.4 Hierarchical Clustering of Segments

Agglomerative hierarchical clustering is a bottom-up clustering algorithm where in each clustering round, two clusters are merged. Algorithm 6 shows the basic flow of the hierarchical clustering algorithm of the Mixed-Bag Solver; it is adapted from [21].

The only inputs to the hierarchical clustering algorithm are the segments found in the segmentation stage and the Segment Overlap Matrix from the Stitching stage.

#### 3.4.1 Calculating the Initial Similarity Matrix

The Segment Overlap Matrix is a form of hollow matrix, where all elements in the matrix, except those along the diagonal, are populated with meaningful values. In contrast, hierarchical clustering merges segments using a triangular, similarity matrix. Equation (3) defines the similarity,  $\omega_{i,j}$  between any two clusters  $\Phi_i$  to  $\Phi_j$ .

$$\omega_{i,j} = \frac{\text{Overlap}(\Phi_i, \Phi_j) + \text{Overlap}(\Phi_j, \Phi_i)}{2} \quad (3)$$

If there are  $n$  solved segments found during segmentation, then the initial

similarity matrix  $\Gamma$  is size  $n$  by  $n$ . Each element in  $\Gamma$  is defined by Equation (4).

Both  $i$  and  $j$  are bounded between 1 and  $n$  inclusive. What is more, all elements in  $\Gamma$  are normalized between 0 and 1, also inclusive.

$$\Gamma = \begin{cases} 0 & j \geq i \\ \omega_{i,j} & i < j \end{cases} \quad (4)$$

### 3.4.2 Updating the Similarity Matrix via Single Linking

The Mixed-Bag Solver uses the Single Link version of hierarchical clustering. Hence, the similarity between any two cluster segments is defined as the similarity between the two most similar segments in either cluster. This approach is required because two segments clusters may only be adjacent along the border of two of the composite segments.

Equation (5) defines the similarity between any a merged cluster containing segment clusters,  $\Sigma_x$  and  $\Sigma_y$ , and any other segment cluster  $\Sigma_z$ . Note that segment  $\Phi_i$  is a member of the union of segment clusters  $\Sigma_x$  and  $\Sigma_y$  while segment  $\Phi_j$  is a member of segment cluster  $\Sigma_z$ .

$$\omega_{x \cup y, z} = \arg \max_{\Phi_i \in (\Sigma_x \cup \Sigma_y)} \left( \arg \max_{\Phi_j \in \Sigma_z} \omega_{i,j} \right) \quad (5)$$

### 3.4.3 Terminating Hierarchical Clustering

Unlike traditional hierarchical clustering, the Mixed-Bag Solver does not always continuing merging the segment clusters until only a cluster remains. Rather, the solver continues clustering until the maximum similarity between any of the

remaining clusters drops below a predefined threshold. In this thesis, a minimum inter-cluster similarity of 0.1 provided sufficient clustering accuracy without merging unrelated segments.

The number of segments clusters remaining at the end of hierarchical clustering represents the expected number of ground-truth images provided to the solver. The segment clusters are then passed to the next stage to determine the final seed pieces for each output puzzle.

### 3.5 Final Seed Piece Selection

Most of the modern jigsaw puzzle solvers [14, 15, 16] rely on a kernel growing model, where a kernel is a partial assembly of one or more pieces. As such, once the Mixed-Bag Solver has determined the expected number of input puzzles via hierarchical clustering, the algorithm then selects the seed piece for each of the output solutions.

In Chapter 2, it was explained that Paikin & Tal require that an output puzzle’s seed piece be “both distinctive and [lie] in a distinctive region.” Their algorithm applies this criteria greedily at run time. Hence, their algorithm often picks suboptimal seeds (e.g., pieces from the same input puzzle are selected as seeds for multiple output puzzles). In contrast, the combination of segmentation and hierarchical clustering in the Mixed-Bag Solver partitions the set of input pieces into disjoint sets, with each set roughly approximating a single solved puzzle. Therefore, the Mixed-Bag Solver selects the seed for each output puzzle from the members of its associated segment cluster. The algorithm uses the same approach as Paikin & Tal wherein the selected seed from the segment cluster is a “piece that is both distinctive and lies in a distinctive region.” However, since this selection is not made greedily

and instead uses the segment clusters, the quality of the selection is superior.

### 3.6 Final Assembly

Once the seed pieces have been selected from the segment clusters, the seeds are used as the initial kernel for the solver outputs. Assembly then proceeds simultaneously across all boards. The fully-assembled boards, with all pieces placed, are the Mixed-Bag Solver’s final output.

## CHAPTER 4

### Quantifying and Visualizing the Quality of a Mixed-Bag Solver Output

Modern jig swap puzzle solvers are not able to perfectly reconstruct the ground-truth input in most cases. As such, quantifiable metrics are required to objectively compare the quality of outputs from different solvers. Cho *et al.* [13] defined two such metrics namely: direct accuracy and neighbor accuracy. These metrics have been used by others including [15, 14, 16, 22, 17]. This section describes the existing quality metrics, their weaknesses, and proposes enhancements to these metrics to make them more meaningful for Type 2 and Mixed-Bag puzzles. This thesis also proposes advanced metrics for quantifying the best buddy attributes of an image.

In the final section, tools developed as part of this thesis to visualize the solver output quality are discussed.

#### 4.1 Direct Accuracy

Direct accuracy is a relatively naïve quality metric; it is defined as the fraction of pieces placed in the same location in both the ground-truth (i.e., original) and solved image with respect to the total number of pieces. Equation (6) shows the formal definition of direct accuracy ( $DA$ ), where  $n$  is the total number of pieces and  $c$  is the number of pieces in the solved image that are placed in their original (i.e., correct) location.

$$DA = \frac{c}{n} \tag{6}$$

Direct accuracy is vulnerable to shifts in the solved image where even a few misplaced pieces can cause a significant decrease in accuracy. As shown in Figure 3, this can be particularly true when the ground-truth image's dimensions are not known by the solver.

This thesis proposes two new direct accuracy metrics namely: Enhanced Direct Accuracy Score (EDAS) and Shiftable Enhanced Direct Accuracy Score (SEDAS). They are described in the following two subsections; the complementary relationship between EDAS and SEDAS is described in the third subsection.

#### 4.1.1 Enhanced Direct Accuracy Score

The standard direct accuracy metric does not account for the possibility that there may be pieces from multiple input puzzles in the same solver output image. For a given a puzzle  $P_i$  in the set of input puzzles  $P$  (i.e.,  $P_i \in P$ ) and a set of solved puzzles  $S$  where  $S_j$  is in  $S$ , Enhanced Direct Accuracy Score (EDAS) is defined as shown in Equation (7).  $c_{ij}$  is the number of pieces from input puzzle  $P_i$  correctly placed (with no rotation for Type 2 puzzles) in solved puzzle  $S_j$  while  $n_i$  is the number of pieces in puzzle  $P_i$ .  $m_{k,j}$  is the number of pieces from an input puzzle  $P_k$  (where  $k \neq i$ ) that are also in  $S_j$ .

$$EDAS_{P_i} = \arg \max_{S_j \in S} \frac{c_{i,j}}{n_i + \sum_{k \neq i} (m_{k,j})} \quad (7)$$

Standard direct accuracy (see Equation (6)) and EDAS are equivalent when solving a single puzzle. For Mixed-Bag solvers, EDAS necessarily marks as incorrect any pieces from  $P_i$  that are not in  $S_j$  by dividing by  $n_i$ . What is more, the summation of  $m_{k,j}$  in EDAS penalizes for any puzzle pieces in the solver output  $S_j$

that are not from input puzzle  $P_i$ . Therefore, EDAS takes into account both extra and missing pieces in the solver output.

It is important to note that EDAS is a score and not a measure of accuracy. While its value is bounded between 0 and 1 (inclusive), it is not specifically defined as the number of correct placements divided by the total number of placements since the denominator of Equation (7) is greater than or equal to the number of pieces in both  $P_i$  and  $S_j$ .

Similar to the standard direct accuracy metric, an image is considered to be “perfectly reconstructed” if it has an EDAS of 1.

#### 4.1.2 Shiftable Enhanced Direct Accuracy Score

As mentioned previously, the direct accuracy decreases if there are shifts in the solved image. In many cases such, direct accuracy is overly punitive.

Figure 3 shows a ground-truth image and an actual solver output when the puzzle boundaries were not fixed. Note that only a single piece is misplaced; this shifted all other pieces to the right one location causing the direct accuracy to drop to zero. Had this same piece been misplaced along either the right or bottom side of the image, the direct accuracy would have been largely unaffected. The fact that direct accuracy can give such vastly differing results for essentially the same error shows that direct accuracy has a fundamental flaw. This thesis proposes Shiftable Enhanced Direct Accuracy Score (SEDAS) to address the often misleadingly punitive nature of standard direct accuracy.

Equation (8) is the formal definition of *SEDAS*.  $d_{min}$  represents the Manhattan distance between the upper left corner of the solved image and the



(a) Ground-Truth Image

### (b) Solver Output

Figure 3: Solver Output where a Single Misplaced Piece Catastrophically Affects the Direct Accuracy

nearest placed puzzle piece. Similarly,  $L$  is the set of all puzzle piece locations within radius  $d_{min}$  (inclusive) of the upper left corner of the image. Given that  $l$  is a location in  $L$  that is used as the reference point for determining the absolute location of all pieces, then SEDAS is defined as shown in Equation (8).

$$SEDAS_{P_i} = \arg \max_{l \in L} \left( \arg \max_{S_j \in S} \frac{c_{i,j,l}}{n_i + \sum_{k \neq i} (m_{k,j})} \right) \quad (8)$$

In the standard definition of direct accuracy proposed by Cho *et al.*,  $l$  is fixed at the upper left corner of the image. In contrast, SEDAS shifts this reference point within a radius of the upper left corner of the image in order to find a more meaningful value for direct accuracy.

Rather than defining SEDAS based off the distance  $d_{min}$ , an alternative approach is to use the point anywhere in the image that maximizes Equation (8). However, that approach can take significantly longer to compute in particular when the solved puzzle has several thousand pieces. SEDAS balances the need for a meaningful direct accuracy score against computation efficiency.

#### 4.1.3 Necessity of Using Both EDAS and SEDAS

While EDAS can be misleadingly punitive, it cannot be wholly replaced by SEDAS. Rather, EDAS and SEDAS serve complementary roles. First, EDAS must necessarily be calculated as part of SEDAS since the upper left corner location is inherently a member of the set  $L$ . Hence, there is no additional time required to calculate EDAS. What is more, by continuing to use EDAS along with SEDAS, some shifts in the solved image may be quantified; this would not be possible if SEDAS was used alone.

## 4.2 Neighbor Accuracy

Cho *et al.* [13] defined neighbor accuracy as the ratio of the number of puzzle piece sides adjacent to the same piece’s side in both the ground-truth and solved image versus the total number of puzzle piece sides. Formally, let  $q$  be the number of sides each piece has (i.e., four in a jig swap puzzle) and  $n$  be the number of pieces. If  $a$  is the number of puzzle piece sides adjacent in both the ground-truth and solved images, then the neighbor accuracy,  $NA$ , is defined as shown in Equation (9).

$$NA = \frac{a}{n q} \tag{9}$$

Unlike direct accuracy, neighbor accuracy is largely unaffected by shifts in the solved image since it considers only a piece’s neighbors and not its absolute location. However, the standard definition of neighbor accuracy cannot encompass the case where pieces from multiple input puzzles may be present in the same solver output.

#### 4.2.1 Enhanced Neighbor Accuracy Score

Enhanced Neighbor Accuracy Score (ENAS) improves the neighbor accuracy metric by providing a framework to quantify the quality of Mixed-Bag solver outputs.

Let  $n_i$  be the number of puzzle pieces in the input puzzle  $P_i$  and  $a_{i,j}$  be the number of puzzle piece sides adjacent in  $P_i$  and  $S_j$ . If  $m_{k,j}$  is the number of puzzle pieces from an input puzzle  $P_k$  (where  $k \neq i$ ) in  $S_j$ , then the ENAS for  $P_i$  is defined as shown in Equation (10).

$$ENAS_{P_i} = \arg \max_{S_j \in S} \frac{a_{i,j}}{q(n_i + \sum_{k \neq i} m_{k,j})} \quad (10)$$

In the same fashion as the technique described for EDAS in Section 4.1.1, ENAS divides by the number of pieces  $n_i$  in input puzzle  $P_i$ . By doing so, it effectively marks as incorrect any pieces from  $P_i$  that are not in  $S_j$ . What is more, by including a summation of all  $m_{k,j}$  in the denominator of (10), ENAS marks as incorrect any pieces not from  $P_i$  that are in  $S_j$ . The combination of these two factors allows ENAS to account for extra and misplaced pieces.

### 4.3 Best Buddy Metrics

Chapter 2 explains that two puzzle pieces are best buddies on their respective sides if they are both more similar to each other than they are to any other pieces. This thesis refers to a best buddy relationship as “adjacent” if the two pieces are neighbors on their respective sides. In contrast, “non-adjacent” best buddies are not neighbors. It is also possible that a piece has no best buddy at all on one or more sides.

Best buddy relationships have been used for segmentation [14],

placement citepaikin 2015, and as an estimation metric [15]. To date, no specific metrics or additional subclassifications of best buddy relationships has been proposed. The following subsections propose new metrics for studying the best buddy profile of both input and solved puzzles.

#### 4.3.1 Interior and Exterior Best Buddies

If an image has fewer non-adjacent best buddies, it means that best buddy relationships become a more accurate determiner of puzzle piece adjacency. It is expected that a pair of best buddies are more likely to be non-adjacent if they are have no neighbor at all (i.e., the piece(s) is next to an open location like the edge of the image). This is because those puzzle piece sides have no true neighbor leaving them more inclined to couple with an unrelated piece, which is often another piece's side with no neighbor. This is illustrated by the example described in Section 4.4.3.

This thesis subcategorizes non-adjacent best buddies depending on whether they are internal (i.e., the piece has an actual neighbor) or external (i.e., the piece has no neighbor). Interior non-adjacent best buddies are generally more concerning since they are used for segmentation and potentially as an estimation metric.

#### 4.3.2 Best Buddy Density

As mentioned previously, each puzzle piece side may or may not have a best buddy relationship. For a puzzle consisting of  $n$  pieces each of which has  $q$  sides<sup>1</sup>, Equation (11) defines the Best Buddy Density (BBD) for an image that has  $b$  total best buddies. BBD is bounded between 0 and 1 (inclusive); a higher best buddy density indicates that the individual puzzle pieces can be more easily differentiated

---

<sup>1</sup>In a jig swap puzzle,  $q$  is equal to 4.

from one another.

$$BBD = \frac{b}{n q} \quad (11)$$

Ideally, a puzzle would have only adjacent best buddies, and that all neighboring puzzle piece sides were also adjacent best buddies. In such cases, the best buddy density would be less than one; the extent to which it would be below one is dependent on the puzzle dimensions as well as the number missing pieces (if any).

Best buddy density may vary across an image with some areas showing lower density than others. Equation (11) can be adjusted to a more local metric by reducing the value of  $b$  and  $n$  based off the best buddy profile of a connected subset of pieces.

#### 4.4 Visualizing Solver Output Quality and Best Buddies Relationships

In images with thousands of pieces, it is often difficult to visually determine the location of individual pieces that are incorrectly placed. What is more, visual tools help developers quickly detect and fix latent bugs. The following two subsections describe the tools developed as part of this thesis for visualizing direct and neighbor accuracy as well as for visualizing best buddies.

##### 4.4.1 Visualizing EDAS and SEDAS

In standard direct accuracy, EDAS, and SEDAS, each puzzle piece is assigned a single value (i.e., correct or incorrect). Due to that, the direct accuracy visualization represents each puzzle by a square filled with a solid color. One additional refinement used in this thesis is to subdivide the “incorrect” placements into a set of subcategories; they are, in order of precedence: wrong puzzle, wrong location, and

Wrong Puzzle	Wrong Location	Wrong Rotation	Correct Location	No Piece Present

Table 1: Color Scheme for Puzzles Pieces in Direct Accuracy Visualizations

wrong rotation. Table 1 shows the colors assigned to puzzle pieces depending on their direct accuracy classification. Assuming no missing pieces in the ground-truth image, the ideal EDAS and SEDAS visualization would have the same dimensions as the ground-truth input and would consist of only green squares.

Figure 4 shows a Type 2 solver output as well as its associated EDAS and SEDAS visualizations. Since four puzzle pieces were erroneously placed on the left of the image, all but one had the wrong location according to EDAS; the only exception is a single piece that had the right location but wrong rotation. In contrast, almost all pieces have the correct location in the SEDAS representation; note that the piece in the correct location but wrong rotation in EDAS has the wrong location in SEDAS.

#### 4.4.2 Visualizing ENAS

In a jig swap puzzle, a piece may have best buddies on up to four sides (since the pieces are square). As such, each piece in the ENAS visualization is divided into four isosceles triangles; the base of each triangle is along the side of the puzzle piece whose neighbor accuracy is being represented. A puzzle piece’s four isosceles triangles all share a common, non-base vertex at the piece’s center. Table 2 defines the color assigned to each triangle depending on whether a piece’s neighbors in the solver output and ground-truth image match. The “wrong puzzle” classification applies only to Mixed-Bag puzzles and occurs when a piece in the solver output is does not

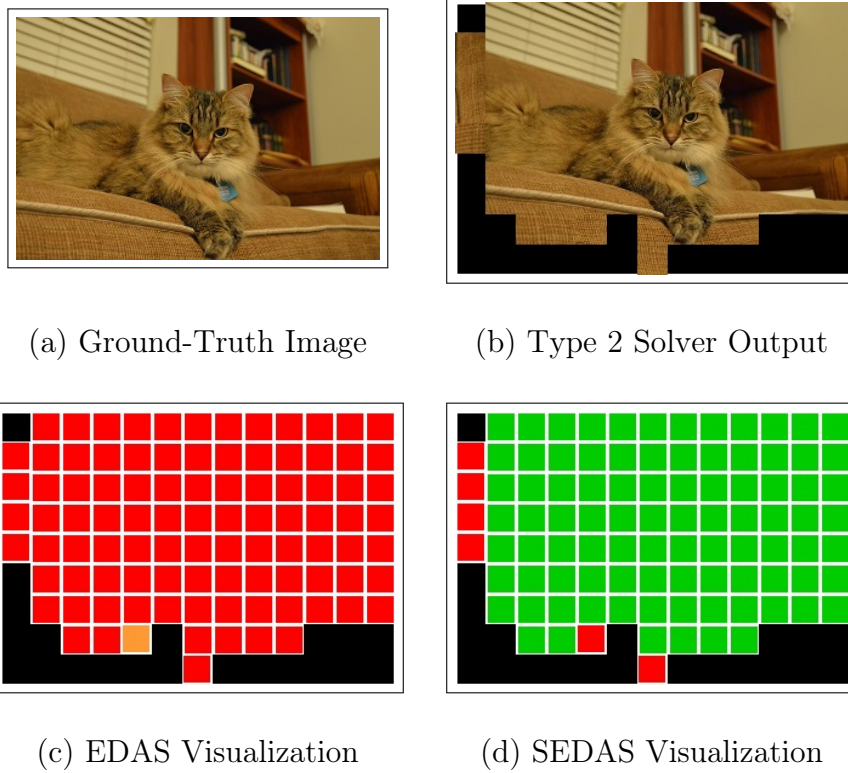


Figure 4: Example Solver Output Visualizations for EDAS and SEDAS

Wrong Puzzle	Wrong Neighbor	Correct Neighbor	No Piece Present
Blue	Red	Green	Black

Table 2: Color Scheme for Puzzles Piece Sides in Neighbor Accuracy Visualizations

from the puzzle of interest,  $P_i$ .

Figure 5 shows an actual output when solving a Mixed-Bag puzzle with two images. Note that that the puzzle of interest ( $P_i$ ) is the glass and stone building while the other puzzle ( $P_k$ ) is a rainforest house.

All pieces that came from the rainforest house image are shown as blue despite being assembled correctly; this is because they are not from the puzzle of interest. All



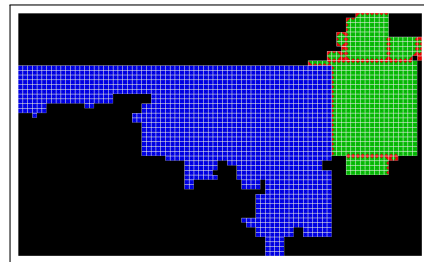
(a) Input Image # 1 -  
Rainforest House [23]



(b) Input Image # 2 - Building  
Exterior [23]



(c) Solver Output



(d) ENAS Visualization

Figure 5: Example Solver Output Visualization for ENAS

neighbors from the puzzle of interest (i.e., the glass and stone building) that are placed next to their original neighbor are represented by green triangles while all incorrect neighbors, such as those bordering the rainforest house image, are represented by red triangles.

#### 4.4.3 Visualizing Best Buddies

The visualization for best buddies is similar to that of neighbor accuracy. Hence, each puzzle piece in the best buddy visualization is divided into four isosceles triangles with each triangle representing the piece’s best buddy relationship with its neighbor. Table 3 defines the color scheme used to denote the three best buddy relationships outlined in Section 4.3.

No Best Buddy	Non-Adjacent Best Buddy	Adjacent Best Buddy	No Piece Present

Table 3: Color Scheme for Puzzles Piece Sides in Best Buddy Visualizations

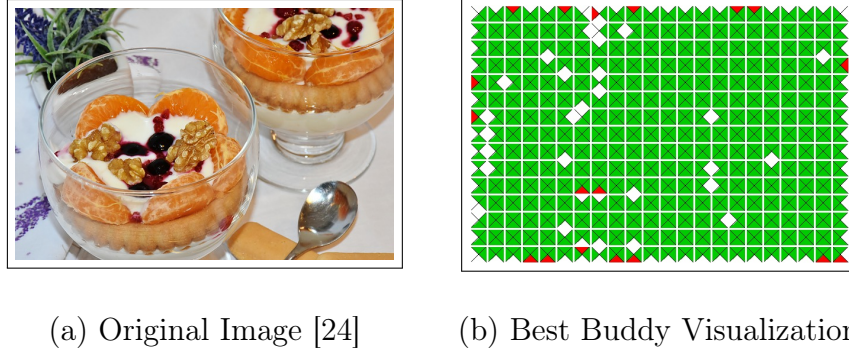


Figure 6: Visualization of Best Buddies in an Image

Figure 6 shows an example image and its associated best buddy visualization. Note that the image has 4 interior and 14 exterior non-adjacent best buddies. This is despite having 16-times more interior interior sides. What is more, one can see that the best buddy density is high and generally uniform.

## CHAPTER 5

### Experimental Results

All experiments in this thesis used a set of standard conditions. First, the length and width of each puzzle piece was set to 28 pixels per the standard established by [13] and subsequently used by [14, 17, 15, 16]. What is more, the Mixed-Bag Solver was passed no information concerning piece location nor rotation. Furthermore, no information concerning the size of the dimensions or number of pieces in each ground-truth image is provided to the solver. Concerning the number of input puzzles, Paikin & Tal’s algorithm requires this information; as such, all runs of their algorithm were supplied this, meaning their algorithm is by definition solving a simpler problem. Despite that, the Mixed-Bag Solver still generally outperforms their algorithm.

To compare the performance of the Mixed-Bag Solver and Paikin & Tal’s algorithm on multiple images, this thesis used Pomeranz *et al.*’s dataset that contains 20 images, each of which 805 pieces. In each test, a specified number of images (ranging from 2 were selected, without replacement from the pool of 20 images. The outputs generated by the two algorithms were then compared. Table 4 shows the number of times the solvers were run with the specified number of puzzles as the input. As explained in Section 3.1.1, the execution time of Paikin & Tal’s assembler can grow cubically, in particular if Best Buddy Density is low. As such, the solver was performed fewer times as the number of input puzzles increased.

# Puzzles	2	3	4	5
# Iterations	55	25	8	5

Table 4: Number of Solver Iterations for Each Puzzle Input Count

### 5.1 Accuracy Determining the Number of Input Puzzles

For the Mixed-Bag Solver to provide meaningful outputs, it must be able to identify the number of ground-truth inputs provided to the solver. The test dataset used to measure the solver’s performance in this area was published by Pomeranz *et al.* in [23]; the dataset consists of 20 images, each of which has 805 pieces.

The next subsection discusses the solver’s performance when provided only a single image. This is separated from the more general discussion as the algorithm’s performance on a single image marks the ceiling of its performance. The algorithm’s performance when solving two to five puzzles is discussed in a separate subsection.

#### 5.1.1 Single Puzzle Solving

The Mixed-Bag solver was able to correctly identify the single ground-truth image for 17 out of the 20 images (i.e., 85% accuracy). For the remaining 3 images, the solver estimated that there were 2 images, meaning the error was at most only a single puzzle. Appendix B shows the ground-truth image as well as the outputs from Paikin & Tal’s algorithm as well as this thesis’ Mixed-Bag Solver.

The Mixed-Bag Solver struggled to correctly identify the number of inputs when the image has large areas with little variation (e.g., a blue sky, smooth water, etc.). Two example images from the test dataset are shown in Figure 7 shows two images in the Pomeranz *et al.*. The Mixed-Bag Solver was able to perfectly reconstruct image (a); in contrast, the Mixed-Bag Solver thought the pieces from

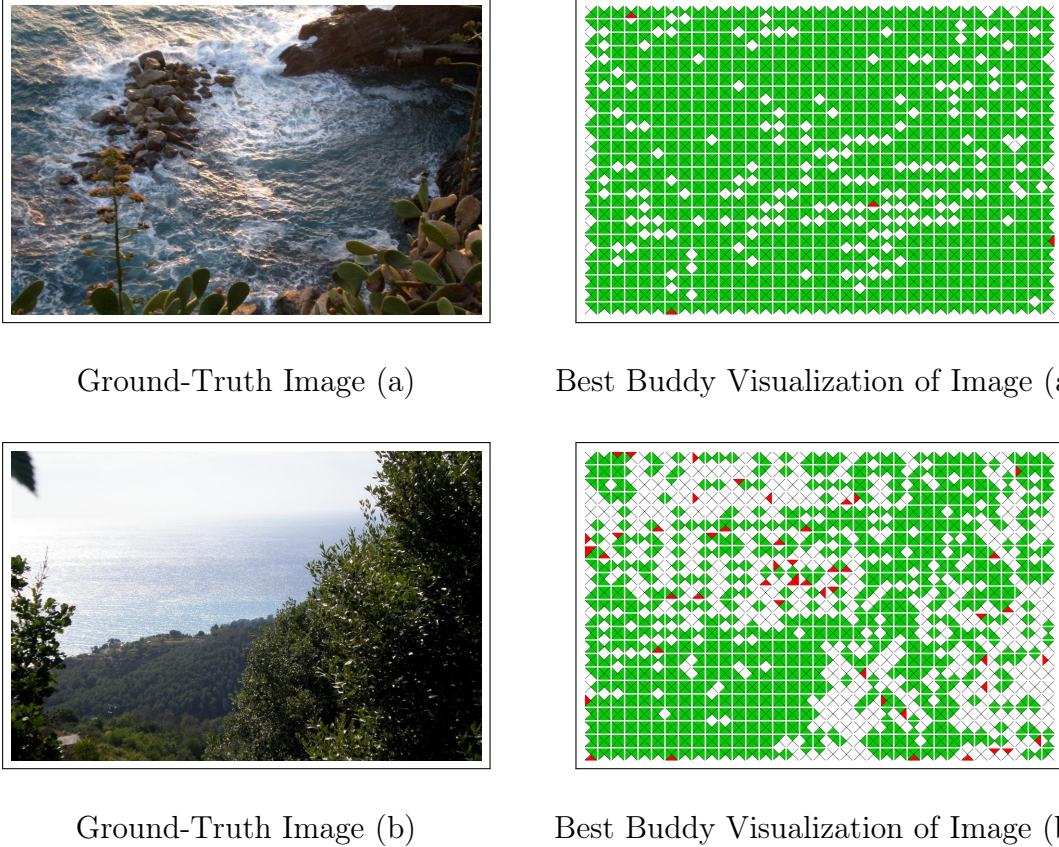


Figure 7: Comparison of Best Buddy Density and Interior Non-Adjacent Best Buddies for Two Images from the Pomeranz *et al.* 805 Piece Dataset

image (b) came from two separate puzzles.<sup>1</sup> The best buddy visualizations in Figure 7 show two images in the Pomeranz *et al.* show that image (a) had a significantly higher best buddy density as well as much fewer interior non-adjacent best buddies. It is these two factors the contributed the most to the Mixed-Bag Solver being unable to determine the number of input images for the three puzzles.

It is important to note that the difficulty the Mixed-Bag Solver has reconstructing images with low Best Buddy Density is actually an artifact of the assembler and not the solver. Paikin & Tal mentioned in [16] that their solver may

---

<sup>1</sup> Appendix B shows the three images that were incorrectly identified by the Mixed-Bag Solver as well as the solver outputs generated.

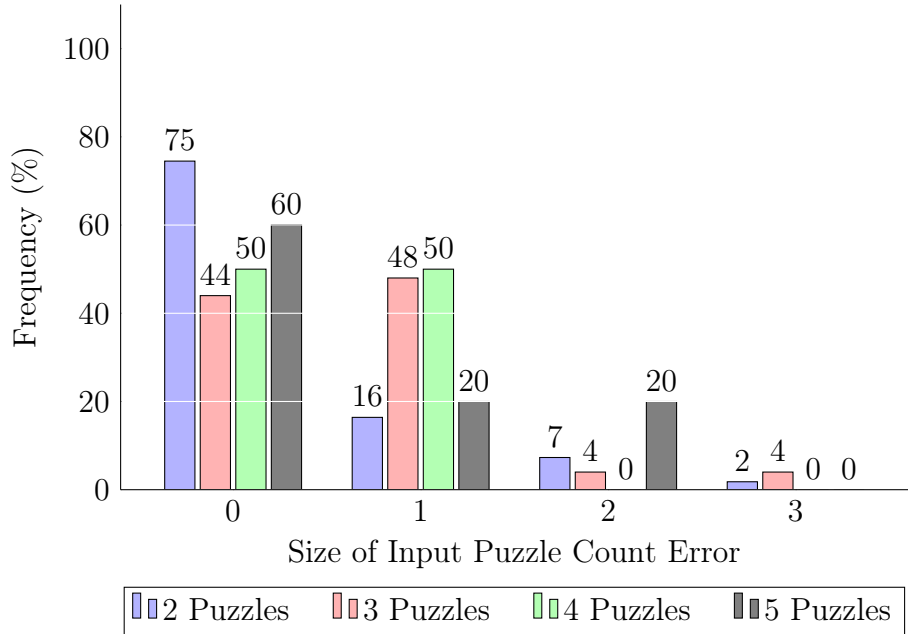


Figure 8: Mixed-Bag Solver’s Input Puzzle Count Error Frequency

yield “unsatisfactory results” on such images.

### 5.1.2 Multiple Puzzle Solving

As mentioned previously, the Mixed-Bag Solver was tested by randomly selecting a specified number of images, without replacement, from Pomeranz *et al.*’s from the 805 piece dataset. In total, Table 4 shows the number of times the solver was run for each input size. Figure 8 illustrates the performance of the Mixed-Bag Solver in determining the number of input. A correct estimation of the number of puzzles would represent an error of “0” in the figure. Similarly, an overestimation of a single puzzle (e.g., the solver identifying four puzzles when only three were provided as an input) would represent an error of “1.” Across all of the experiments, the Mixed-Bag Solver never underestimated the number of input puzzles; what is more, it never overestimated the number of input puzzles by more than 3.

# of Puzzle	Average SEDAS			Average ENAS			Perfect Reconstruction		
	MBS†	MBS‡	Paikin	MBS†	MBS‡	Paikin	MBS†	MBS‡	Paikin
2	0.850	0.757	0.321	0.933	0.874	0.462	29.3%	23.6%	5.5%
3	0.953	0.800	0.203	0.955	0.869	0.364	18.5%	18.8%	1.4%
4	0.881	0.778	0.109	0.920	0.862	0.260	25.0%	15.6%	0%
5	0.793	0.828	0.099	0.868	0.877	0.204	20.0%	24%	0%

Table 5: Comparison of Mixed-Bag and Paikin & Tal Solvers Performance on Multiple Input Puzzles

In this set of experiments, the Mixed-Bag solver correctly determined the number of input puzzles in 65% of the tests. Likewise, in less than 8% of the tests did the solver overestimate the number of input puzzles by more than one. Since the solver never underestimated the number of input puzzles, it is clearly that the solver is over-rejecting the merger of cluster and/or creating very small clusters that are too isolated to merge with the main cluster. It is expected that the performance of the solver would be improved by reducing the minimum clustering threshold (see Section 3.4) as well as increasing the minimum segment size (see Section 3.2.2).

## 5.2 Comparison of Solver Output Quality

As mentioned at the beginning of this chapter, images were randomly selected from the Pomeranz *et al.* dataset and provided to the Mixed-Bag Solver as well as Paikin & Tal’s algorithm. Table 5 and Figure 9 show the quantified quality of the outputs generated by both solvers for varying input puzzle counts. The three metrics used are the Shiftable Enhanced Direct Accuracy Score (SEDAS), Enhanced Neighbor Accuracy Score (ENAS), and the percentage of puzzles assembled perfectly (i.e., input and output puzzles are an identical match). Note that the mean values of SEDAS and ENAS are displayed in the table and graphs; these means will calculated

for all images that among the specified subset of solutions. What is more, the results for the Mixed-Bag Solver (MBS) are subdivided between the case when the number of input puzzles was correctly determined (denoted with a “†” in the table heading) versus all solver results (denoted with a “‡”). This distinction is made since the solver accuracy when correctly identifying the number input puzzles represents the performance ceiling if the hierarchical clustering were optimal.

Across all quality metrics and categories, the Mixed-Bag Solver significantly outperformed Paikin & Tal’ algorithm. This is despite the fact that only Paikin & Tal’s algorithm was provided additional information concerning the number of input puzzles. What is more, unlike Paikin & Tal’s algorithm, the Mixed Bag Solver saw no significant decrease in solver quality as the number of input puzzles were increased. In addition, the Mixed-Bag Solver did not see a substantial difference in solution quality if it incorrectly estimated the number of input images; this indicates that these extra puzzles were relatively insignificant in size since they did not meaningfully affect SEDAS or ENAS.

### 5.3 Ten Puzzle Solving

Paikin & Tal’s [16] algorithm was shown to be able to solve up to five images simultaneously, which represents the most in the current literature. To achieve this, their solver needed to be supplied with the number of input puzzles. In contrast, this Mixed-Bag Solver has been shown to be able to solve up to ten puzzles of varying size. Appendix C shows the input puzzles as well as the Mixed-Bag Solver’s outputs. When the identical set of puzzles were supplied to Paikin & Tal’s algorithm, the seeds for nine of the puzzles came from just three of the input puzzles.

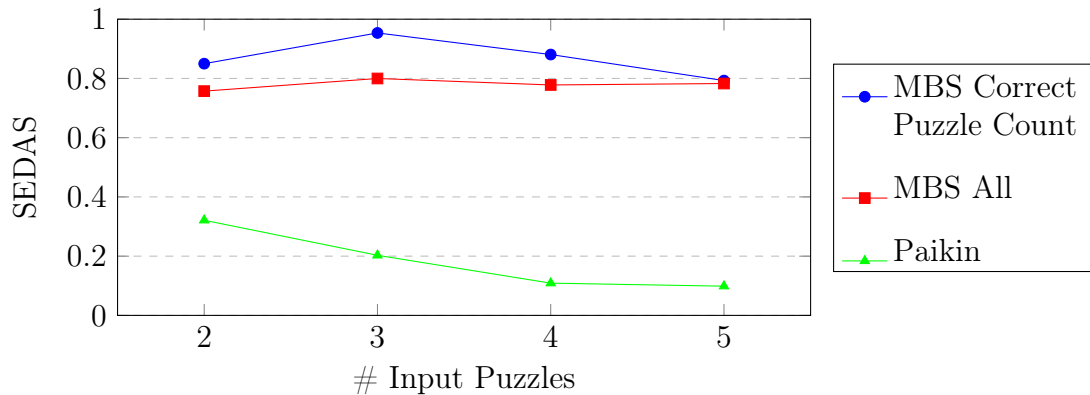
Table 6 shows a comparison of the results between this thesis’ Mixed-Bag

Image		Shifted		SEDAS		ENAS	
ID	# Pieces	MBS	Paikin	MBS	Paikin	MBS	Paikin
(a)	264	No	Yes	1.000	0.000	1.000	0.544
(b)	330	No	Yes	1.000	0.000	1.000	0.090
(c)	432	Yes	Yes	0.905	0.000	0.911	0.034
(d)	540	No	No	0.978	0.526	0.975	0.509
(e)	540	No	No	1.000	0.059	1.000	0.327
(f)	540	Yes	No	0.978	0.943	0.917	0.931
(g)	805	No	Yes	0.997	0.000	0.990	0.077
(h)	805	Yes	Yes	0.958	0.000	0.967	0.070
(i)	805	No	Yes	1.000	0.000	1.000	0.311
(j)	805	Yes	Yes	0.998	0.000	0.990	0.073

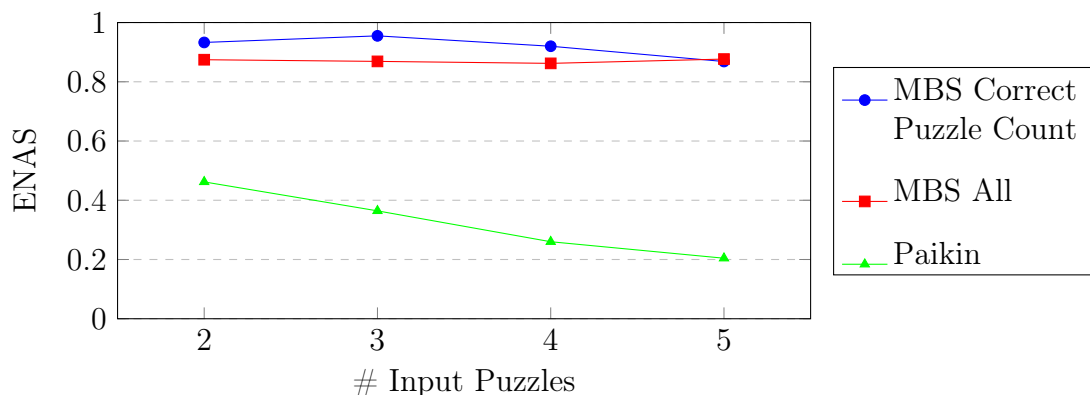
Table 6: Comparison of the Image Shifting, SEDAS, and ENAS Results for the 10 Puzzle Dataset

Solver (MBS) and Paikin & Tal’s algorithm’s. Despite the Mixed-Bag Solver receiving less information, it significantly outperformed Paikin & Tal receiving greater than 90% accuracy for both Shiftable Enhanced Direct Accuracy Score (SEDAS), and the Enhanced Neighbor Accuracy Score (ENAS) on all puzzles. In contrast, Paikin & Tal only exceeded 90% SEDAS and ENAS for image (f).

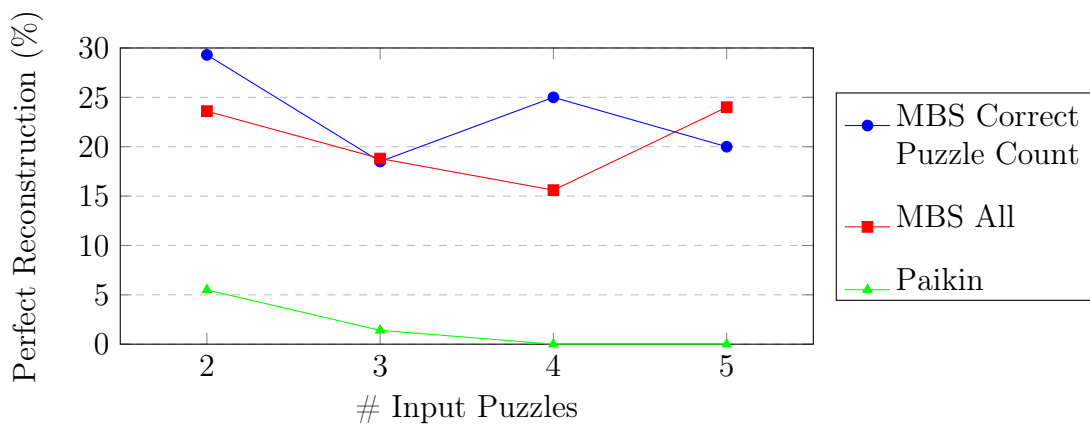
With respect to the unshifted, Enhanced Direct Accuracy Score (EDAS) metric, only four of the Mixed-Bag’s solver outputs showed a shift that would affect EDAS while 7 of Paikin & Tal’s outputs were shifted. This indicates that the Mixed-Bag Solver has a much greater immunity to shifts than Paikin & Tal’s algorithm.



(a) Shiftable Enhanced Direct Accuracy Score (SEDAS)



(b) Enhanced Neighbor Accuracy Score (ENAS)



(c) Percentage of Puzzles Perfectly Reconstructed

Figure 9: Performance of the Mixed-Bag and Paikin & Tal Solvers with Multiple Input Puzzles

## CHAPTER 6

### Conclusions and Future Work

This thesis presented a fully-automated solver for Mixed-Bag jigsaw puzzles. No other solver today has formalized an algorithm estimate the number of input images; what is more, the algorithm has been shown to be able to successfully solve twice as many puzzles as the current state, despite receiving less information. What is more, the solver does not rely on a specific assembly strategy, meaning the solver's performance will improve as better solvers are proposed.

Opportunities currently exist to further improve the Mixed-Bag Solver's performance. First, the ceiling on the quality of solved outputs is significantly affected by the assembler. This solver was designed to be largely independent of the assembler used, meaning the solver's performance will improve as better solvers are proposed. As such, an improved solver that further prioritizes assembly based off best buddies is currently under development. What is more, Paikin & Tal's algorithm often poorly assembles areas with low best buddy density, which this new assembler should also improve.

Another area where future investigation is planned is the threshold for hierarchical clustering, which is currently set at a fixed value. It is expected that a more dynamic approach may improve the clustering overall.

One final area where further work is planned is around the selection of seed pieces. As explained in Section 3.3.2, a stitching piece is by definition a member of a saved segment. In some cases, the mini-assembly may not actually expand the segment, which would in turn prevent segment clustering. An improved approach

may involve selecting stitching pieces that belong to no segment, with the expectation that such pieces may have superior stitching properties.

## LIST OF REFERENCES

- [1] A. D. Williams, *Jigsaw Puzzles: An Illustrated History and Price Guide*. Wallace-Homestead Book Co., 1990.
- [2] A. D. Williams, *The Jigsaw Puzzle: Piecing Together a History*. Berkley Books, 2004.
- [3] H. Freeman and L. Gardner, “Apictorial jigsaw puzzles: The computer solution of a problem in pattern recognition,” *IEEE Transactions on Electronic Computers*, vol. 13, pp. 118–127, 1964.
- [4] T. Altman, “Solving the jigsaw puzzle problem in linear time,” *Applied Artificial Intelligence*, vol. 3, no. 4, pp. 453–462, Jan. 1990.
- [5] E. D. Demaine and M. L. Demaine, “Jigsaw puzzles, edge matching, and polyomino packing: Connections and complexity,” *Graphs and Combinatorics*, vol. 23 (Supplement), pp. 195–208, June 2007.
- [6] B. J. Brown, C. Toler-Franklin, D. Nehab, M. Burns, D. Dobkin, A. Vlachopoulos, C. Doumas, S. Rusinkiewicz, and T. Weyrich, “A system for high-volume acquisition and matching of fresco fragments: Reassembling Theran wall paintings,” *ACM Transactions on Graphics*, vol. 27, no. 3, Aug. 2008.
- [7] M. L. David Koller, “Computer-aided reconstruction and new matches in the Forma Urbis Romae,” *Bullettino Della Commissione Archeologica Comunale di Roma*, vol. 2, pp. 103–125, 2006.
- [8] S. L. Garfinkel, “Digital forensics research: The next 10 years,” *Digital Investigation*, vol. 7, Aug. 2010.
- [9] T. S. Cho, M. Butman, S. Avidan, and W. T. Freeman, “The patch transform and its applications to image editing,” *Proceedings of the 2008 IEEE Conference on Computer Vision and Pattern Recognition (CVPR)*, 2008.
- [10] L. Zhu, Z. Zhou, and D. Hu, “Globally consistent reconstruction of ripped-up documents,” *IEEE Transactions on Pattern Analysis and Machine Intelligence*, vol. 30, pp. 1–13, 2008.
- [11] W. Marande and G. Burger, “Mitochondrial DNA as a genomic jigsaw puzzle,” *Science*, vol. 318, no. 5849, pp. 415–415, 2007.

- [12] Y.-X. Zhao, M.-C. Su, Z.-L. Chou, and J. Lee, “A puzzle solver and its application in speech descrambling,” in *Proceedings of the 2007 International Conference on Computer Engineering and Applications*. World Scientific and Engineering Academy and Society, 2007, pp. 171–176.
- [13] T. S. Cho, S. Avidan, and W. T. Freeman, “A probabilistic image jigsaw puzzle solver,” in *Proceedings of the 2010 IEEE Conference on Computer Vision and Pattern Recognition (CVPR)*, ser. CVPR ’10. IEEE Computer Society, 2010, pp. 183–190.
- [14] D. Pomeranz, M. Shemesh, and O. Ben-Shahar, “A fully automated greedy square jigsaw puzzle solver,” in *Proceedings of the 2011 IEEE Conference on Computer Vision and Pattern Recognition (CVPR)*, ser. CVPR ’11. IEEE Computer Society, 2011, pp. 9–16.
- [15] D. Sholomon, O. David, and N. S. Netanyahu, “A genetic algorithm-based solver for very large jigsaw puzzles,” in *Proceedings of the 2013 IEEE Conference on Computer Vision and Pattern Recognition (CVPR)*, ser. CVPR ’13. IEEE Computer Society, 2013, pp. 1767–1774.
- [16] G. Paikin and A. Tal, “Solving multiple square jigsaw puzzles with missing pieces,” in *Proceedings of the 2015 IEEE Conference on Computer Vision and Pattern Recognition (CVPR)*, ser. CVPR ’15. IEEE Computer Society, 2015.
- [17] A. C. Gallagher, “Jigsaw puzzles with pieces of unknown orientation,” in *Proceedings of the 2012 IEEE Conference on Computer Vision and Pattern Recognition (CVPR)*, ser. CVPR ’12. IEEE Computer Society, 2012, pp. 382–389.
- [18] D. Sholomon, O. David, and N. S. Netanyahu, “Datasets of larger images and GA-based solver’s results on these and other sets,” <http://u.cs.biu.ac.il/~nathan/Jigsaw/>, 2013, (Accessed on 05/01/2016).
- [19] P. S. Foundation, “Comparing python to other languages | python.org,” <https://www.python.org/doc/essays/comparisons/>, (Accessed on 10/09/2016).
- [20] T. H. Cormen, C. E. Leiserson, R. L. Rivest, and C. Stein, *Introduction to Algorithms, Third Edition*, 3rd ed. The MIT Press, 2009.
- [21] P.-N. Tan, M. Steinbach, and V. Kumar, *Introduction to Data Mining, (First Edition)*. Boston, MA, USA: Addison-Wesley Longman Publishing Co., Inc., 2005.
- [22] K. Son, J. Hays, and D. B. Cooper, “Solving square jigsaw puzzles with loop constraints,” in *Proceedings of the 2014 European Conference on Computer Vision (ECCV)*. Springer, 2014, pp. 32–46.

- [23] D. Pomeranz, M. Shemesh, and O. Ben-Shahar, “Computational jigsaw puzzle solving,” [https://www.cs.bgu.ac.il/~icvl/icvl\\_projects/automatic-jigsaw-puzzle-solving/](https://www.cs.bgu.ac.il/~icvl/icvl_projects/automatic-jigsaw-puzzle-solving/), 2011, (Accessed on 05/01/2016).
- [24] H. Braxmeier and S. Steinberger, “Pixabay,” <https://pixabay.com/>, (Accessed on 05/15/2016).

## APPENDIX A

### Example Output of a Single Segmentation Round

This appendix is provided as example to assist in visualizing the different outputs generated during segmentation. Figure A.10 shows the two ground-truth images that were provided to the Mixed-Bag Solver for this example. As explained in Section 3.2, the Mixed-Bag solver assembles the pieces from these images as if they had come from a single puzzle; the assembler output for the first round of segmentation is shown in Figure A.11.

The segments present in the assembler output are shown in Figure A.12, with the segments colored to make them easier to identify. For a given segment, the pieces that are further away from an open location are lighter in color while those closer to a boundary are darker. The stitching pieces that would have resulted from each segment (assuming it exceeded the minimum segment size) are marked with white crosses.

Figure A.13 is the best buddy visualization of the assembler output. Note that the right and left sides of image (a) have stripes of best buddies that extend only in the horizontal direction. As such, each piece in those stripes represent articulation pieces. As such, they were trimmed from the main segment in the center of the image as described in Section 3.2.3.



Image (a) – 805 Pieces



Image (b) – 540 Pieces

Figure A.10: Ground-Truth Images Used in the Segmentation Example

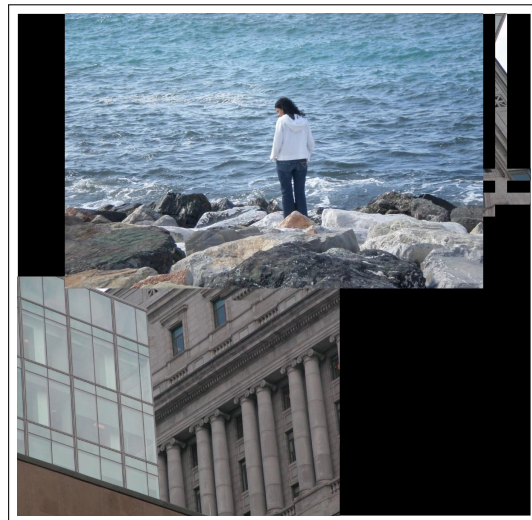


Figure A.11: Example Assembler Output of a Single Puzzle after the First Segmentation Round

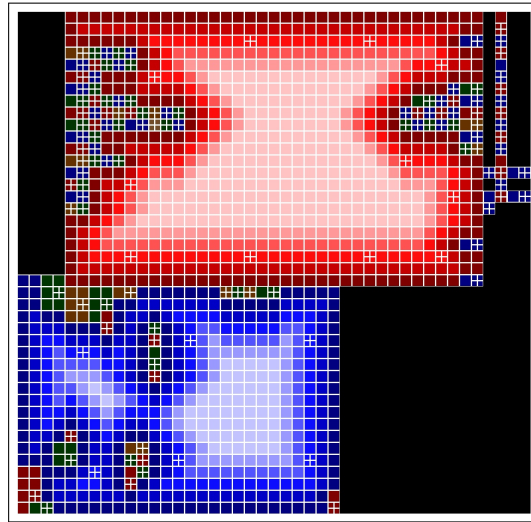


Figure A.12: Segmentation of the Assembler Output with Coloring for Distance to the Nearest Open and Marking of the Articulation Points

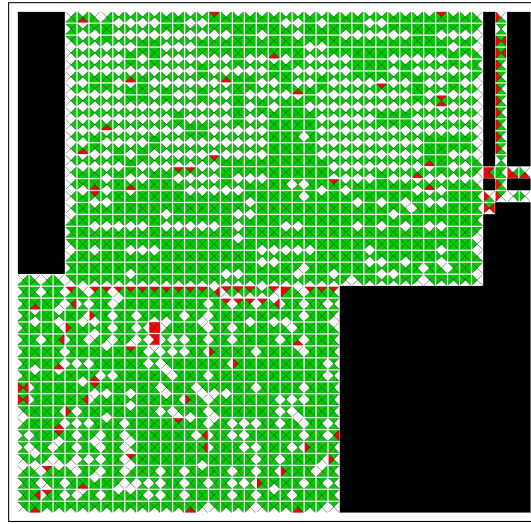


Figure A.13: Best Buddy Visualization of the Assembler Output

## APPENDIX B

### Incorrectly Classified Single Puzzle Images

The Mixed-Bag Solver’s ability to determine the number of ground-truth images passed to the solver was tested using the Pomeranz *et al.* dataset [23] containing 20 images each with 805 pieces. This test measures the performance ceiling of the solver to determine the number of input puzzles.

The Mixed-Bag Solver (MBS) correctly identified that was only a single ground-truth input for 17 out of the 20 images. Figure B.14 shows the three images that the Mixed-Bag Solver were unable to identify being a single image. Figure B.15 contains the Mixed-Bag Solver’s output for these images; clearly, the solver struggled with the large areas of the image where there was little variation (e.g., blue sky, smooth water). Paikin & Tal note in [16] that their assembler does not perform well on such images. Therefore, it is expected the Mixed-Bag Solver’s performance on these images may have improved had a different assembler been used.



Input Image (a)



Input Image (b)

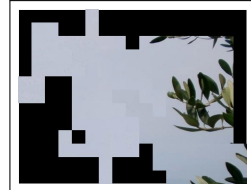


Input Image (c)

Figure B.14: 805 Piece Images that were Incorrectly Identified by the Mixed Bag Solver



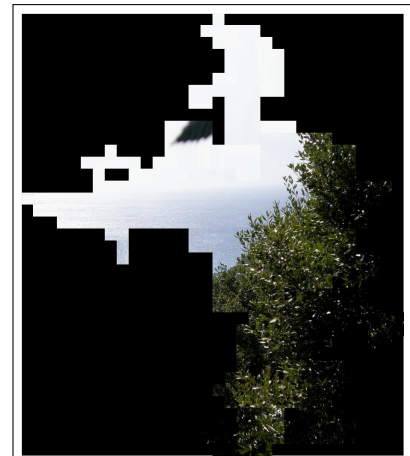
MBS Output (a1)



MBS Output (a2)



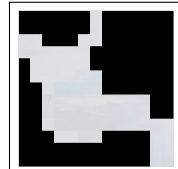
MBS Output (b1)



MBS Output (b2)



MBS Output (c1)



MBS Output (c2)

Figure B.15: Multi-Bag Solver Outputs for the Images not Correctly Identified as Single Inputs

## APPENDIX C

### Ten Puzzle Results

Paikin & Tal [16] showed the results solving a maximum of five puzzles; what is more, they also provided the solver with the number of input puzzles. The Mixed-Bag Solver has shown that it can assemble up to 10 puzzles with results comparable to the Paikin & Tal solver on each image individually.

Figures C.16 and C.17 show the input images supplied to both the Mixed-Bag and Paikin & Tal solvers. The 5,850 pieces come from images that are five different sizes.

Figures C.18 and C.19 show the Mixed-Bag Solver outputs for these images. Four output images (e.g., images (a), (b), (e), (i)) perfectly match their original images. The rest have only have a small percentage of pieces out of place. This is shown in the SEDAS visualizations in Figures C.20 and C.21.



Image (a) – 264 Pieces [24]



Image (b) – 330 Pieces [24]



Image (c) – 432 Pieces [13]



Image (d) – 540 Pieces [23]



Image (e) – 540 Pieces [23]



Image (f) – 540 Pieces [23]

Figure C.16: First Set of Six Images Comprising the 10 Image Test Set



Image (g) – 805 Pieces [23]



Image (h) – 805 Pieces [23]



Image (i) – 805 Pieces [23]



Image (j) – 805 Pieces [23]

Figure C.17: Second Set of Four Images Comprising the 10 Image Test Set



Reconstructed Image (a)



Reconstructed Image (b)



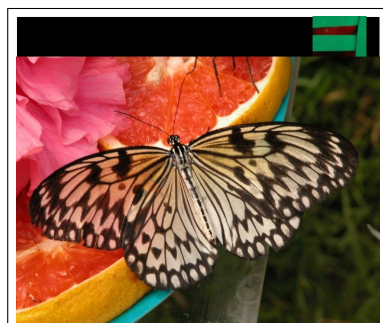
Reconstructed Image (c)



Reconstructed Image (d)



Reconstructed Image (e)



Reconstructed Image (f)

Figure C.18: First Set of Six Mixed-Bag Solver Images for the 10 Image Test Set



Reconstructed Image (g)



Reconstructed Image (h)

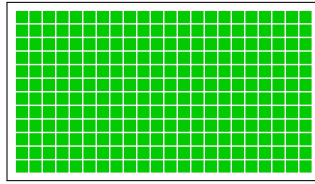


Reconstructed Image (i)

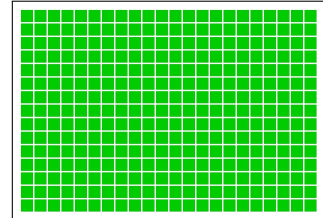


Reconstructed Image (j)

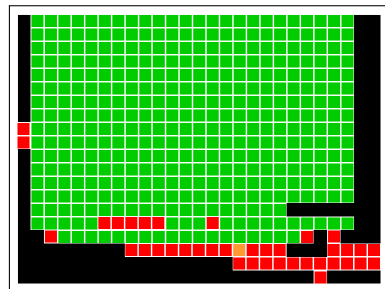
Figure C.19: Second Set of Four Mixed-Bag Solver Images for the 10 Image Test Set



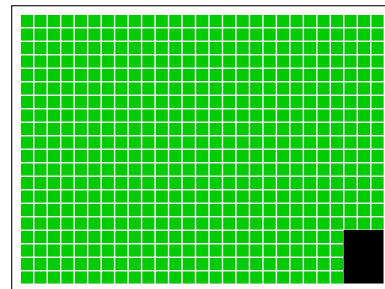
SEDAS Visualization of Image (a)



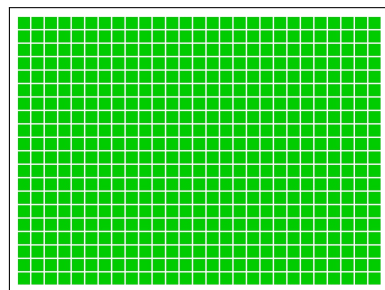
SEDAS Visualization of Image (b)



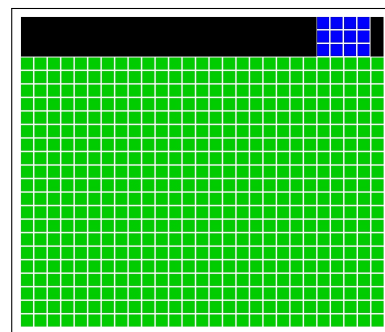
SEDAS Visualization of Image (c)



SEDAS Visualization of Image (d)

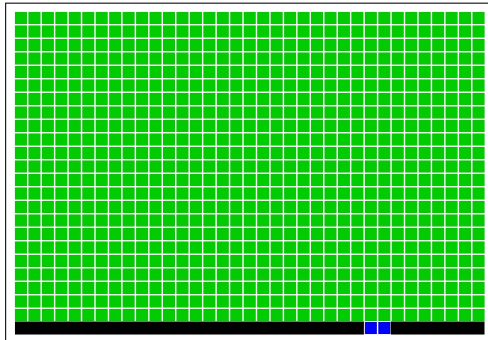


SEDAS Visualization of Image (e)

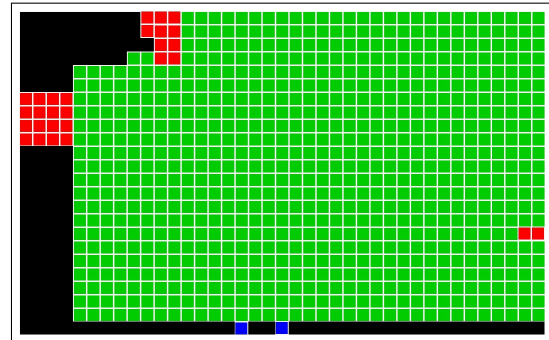


SEDAS Visualization of Image (f)

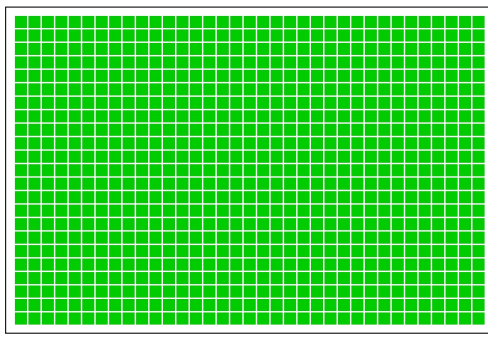
Figure C.20: First Set of Six SEDAS Visualizations for the 10 Image Test Set



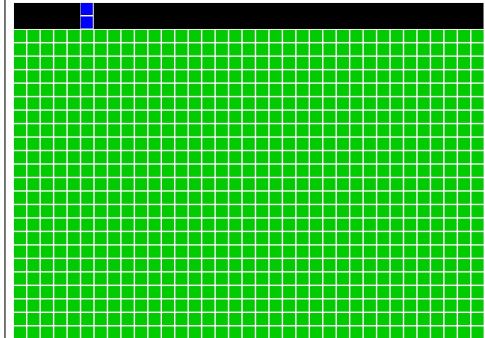
SEDAS Visualization of Image (g)



SEDAS Visualization of Image (h)



SEDAS Visualization of Image (i)



SEDAS Visualization of Image (j)

Figure C.21: Second Set of Four SEDAS Visualizations for the 10 Image Test Set